Available online at www.sciencedirect.com
ScienceDirect
Applied Catalysis B: Environmental 80 (2008) 168–175
APPLIED CATALYSIS B: ENVIRONMENTAL
www.elsevier.com/locate/apcatb

Influence of TiO_2 concentration on the synergistic effect between photocatalysis and high-frequency ultrasound for organic pollutant mineralization in water

Ricardo A. Torres [a,b,c], Jessica I. Nieto [c], Evelyne Combet [b], Christian Pétrier [b], Cesar Pulgarin [c,*]

[a] *Grupo de Electroquímica, Instituto de Química, Facultad de Ciencias Exactas y Naturales, Universidad de Antioquia, A. A. 1226 Medellín, Colombia*
[b] *Université de Savoie, 73376 Le Bourget-du-Lac, France*
[c] *Groupe de Génie Électrochimique, Institut des Sciences et Ingénierie Chimique, Ecole Polytechnique Fédérale de Lausanne, CH-1015 Lausanne, Switzerland*

Received 16 August 2007; received in revised form 5 November 2007; accepted 11 November 2007
Available online 22 November 2007

Abstract

This work deals with the coupling of sonolysis (300 kHz, 80 W) and solar photocatalysis using titanium dioxide, two advanced oxidation processes for the degradation of a model organic pollutant, bisphenol A (BPA). Initially, the performances of the two separate processes in both the elimination and mineralization of BPA were compared. Even if identical BPA byproducts were formed, the two processes were complementary, while ultrasound was better able to eliminate the target pollutant, photocatalysis proved to be more efficient for reaching mineralization. Using the combined system, an interesting synergistic effect, which depends on the titanium dioxide loading, was observed for BPA mineralization. The best synergistic effect was found at low catalyst loading. After 4 h of combined treatment using 0.05 g L^{-1} of titanium dioxide, 62% of dissolved organic carbon (DOC) was eliminated. In contrast, 6 or 12% of DOC was removed by ultrasound alone or photocatalysis alone, respectively. Using 1 g L^{-1} of catalyst, 68 or 50% of DOC was removed by ultrasound/photocatalysis or photocatalysis, respectively. The poor synergistic effect at this catalyst loading can be explained by an inhibiting effect of the titanium dioxide on the cavitational activity.

Keywords: Sonochemical degradation; Photocatalysis; Sonophotocatalysis; Endocrine disrupting chemical; Bisphenol A elimination; Water treatment; Advanced oxidation

1. Introduction

In recent years, there has been increasing interest in the application of advanced oxidation processes (AOPs) as attractive alternative treatments for contaminated ground, surface, and wastewaters containing anthropogenic toxins with low biodegradability, as well as for the purification and disinfection of drinking water [1–3]. AOPs are all based on the production of $^{\bullet}OH$ radicals. These radicals are extraordinarily reactive species that attack most organic molecules, with rate constants usually on the order of 10^6 to 10^9 mol L^{-1} s^{-1} [4]. Interestingly, AOPs offer different routes to $^{\bullet}OH$ radical production, allowing easier tailoring of the process for specific treatment requirements.

Although AOPs have been successfully used for the elimination of a huge number of organic compounds, AOPs cannot achieve complete mineralization of pollutants in several cases due to economical or technical reasons. Thus, in recent years efforts have been made to develop systems combining two different AOPs [5,6] or an AOP with a biological process [7,8].

Among the existing AOPs, sonochemical oxidation has received considerable attention because of its particular efficacy toward volatile and/or hydrophobic compounds [9,10]. Ultrasound irradiation of aqueous solutions leads to acoustic cavitation, i.e., the cyclic formation, growth and

* Corresponding author. Tel.: +41 21 693 47 20; fax: +41 21 693 56 90.
E-mail address: cesar.pulgarin@epfl.ch (C. Pulgarin).

0926-3373/$ – see front matter © 2007 Elsevier B.V. All rights reserved.
doi:10.1016/j.apcatb.2007.11.013

adiabatic implosion of microbubbles. Under these conditions, organic substances with an elevated fugacity character are pyrolysed [11], while non-volatile compounds are degraded by hydroxyl radicals coming from water and oxygen dissociation [12]. Hydrophobic substrates are mainly degraded at the interface of bubbles and solution. Because of the short lifetime of $^{\bullet}$OH radicals, a large fraction recombine at the interface of the bubble before reacting with hydrophilic substances. Thus, polar organic compounds are eliminated in the solution bulk, to a much lower extent than volatile and hydrophobic substrates [13].

TiO_2 photocatalysis is another AOP that has gained considerable attention as a means for water remediation [14,15]. In this process, UV light ($\lambda \leq 387$ nm) is used to excite an electron from the TiO_2 valence band to the conduction band to produce an electron–hole pair. Oxygen dissolved in solution can scavenge excited electrons, limiting the electron–hole recombination. Organic compounds may suffer oxidation directly at the hole. The hole can also undergo charge transfer with adsorbed water molecules or with surface-bound hydroxide species, forming $^{\bullet}$OH radicals. Those organics that remain near the catalyst surface, i.e., highly polar substances, are more likely to be oxidized by photocatalysis.

Enhancement of the photocatalysis efficiency using low-frequency ultrasound (20–100 kHz) has been widely investigated [16–19]. However, in spite of the notable performance of high-frequency ultrasound (frequencies >100 kHz) for degrading organic compounds, fewer reports have addressed the combination of photocatalysis and high-frequency ultrasound. Moreover, the synergistic effect between these two processes is a controversial matter. Stock et al. [20] recently reported that, after 4 h of treatment using a combined high-frequency ultrasound/photocatalysis system, the mineralization rate of an azo dye was greater than that resulting from an additive effect of the individual AOPs. In contrast, Théron et al. [16], studying the degradation of phenyltrifluoromethylketone, reported the absence of synergy between the same two AOPs.

The aim of this work is to contribute to the understanding of the synergistic effect between TiO_2 photocatalysis and high-frequency ultrasound for the degradation and mineralization of organic pollutants. Bisphenol A [BPA: 2,2-bis(4-hydroxyphenyl)propane] was selected as the target compound because it is an endocrine disrupting chemical widely used in the plastic industry as a monomer for production of epoxy resins and polycarbonate. This compound is released into the environment from bottles, packaging, landfill leachates, paper, and plastics plants [21–23]. Previous reports have shown that BPA treatments with classical chemical processes, such as chlorination, lead to products with even higher endocrine disrupting effects and/or toxicity [24–26].

2. Experimental

2.1. Reagents

Bisphenol A and ammonium heptamolybdate were obtained from Aldrich. Potassium iodide, acetic acid, and sulfuric acid were supplied by Fluka. Potassium hydrogen phthalate and acetonitrile were purchased from Merck and Fisher Chemicals, respectively. All these chemicals were used without any further purification. Throughout the experiments, oxygen was added to the system. Oxygen was selected as saturating gas instead of air in order to avoid the formation of nitrite and nitrate ions during sonication of aqueous solutions [5], and because of its excellent performance in ultrasound water treatments [27,28].

Milli-Q water was used throughout, for the preparation of aqueous solutions and as a component of the mobile phase in HPLC analysis.

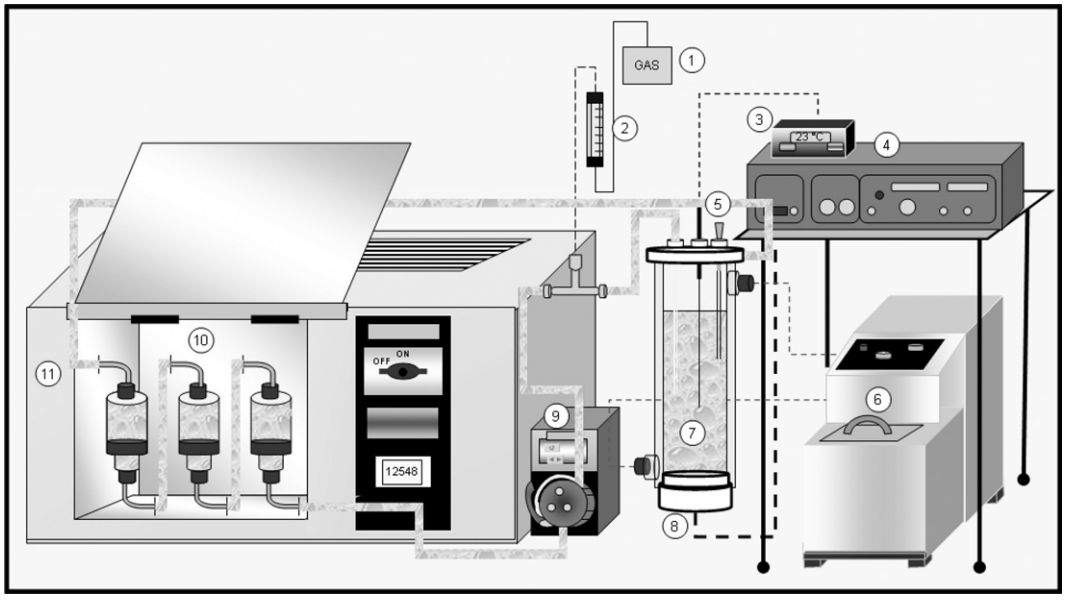

Fig. 1. Sonochemical/photocatalysis reactor used for the BPA treatment. Numbers in circles define the following: (1) Gas container; (2) gas flow control; (3) temperature control; (4) ultrasound generator; (5) sampling; (6) thermostatic bath; (7) sonochemical reactor; (8) piezo-electric disc; (9) peristaltic pump; (10) Pyrex vessels; (11) solar simulator.

2.2. Apparatus

All the experiments were carried out with 600 mL of a BPA 118 μmol L^{-1} solution at pH 3, in two separate systems, one under sonication and the other one under suntest irradiation (Fig. 1).

To keep a constant temperature (22 ± 2 °C) the sonochemical system was a cylindrical glass water-jacketed reactor (capacity 500 mL). Ultrasonic waves (300 kHz and 80 W) were emitted from the bottom of the reactor through a piezo-electric disc (diameter 4 cm) fixed on a Pyrex plate (diameter 5 cm) [29]. Ultrasonic energy dissipated in the reactor (∼50% of the electrical power used) was estimated by the calorimetric method [30].

The photochemical reactor consisted of three serial Pyrex glass vessels, each one having an illuminated volume of 50 mL. The Pyrex vessels were illuminated from the outside using a solar lamp CPS Suntest system (Atlas Gmbh) with a radiation intensity of 830 W m^{-2}. This lamp has a spectral distribution with about 0.5% of the emitted photons at wavelengths shorter than 300 nm and about 7% between 300 and 400 nm. The emission spectrum between 400 and 800 nm follows the solar spectrum. A peristaltic pump recirculated the solutions from the sonochemical reactor to the photochemical reactors with a flow rate of 230 mL min^{-1}. The total volume of the solution (600 mL) was distributed in three parts: 300 mL in the sonochemical vessel, 150 mL in the photochemical system and the rest (150 mL) in the connecting tubing. Using this configuration, we tested the coupling of the two AOPs in a sequential mode. We also tested each system, ultrasound or TiO_2 photocatalysis, acting separately. In a typical photocatalysis or ultrasound/photocatalysis run, the appropriate quantity of TiO_2 was added in the reaction mixture and the suspension was left for 4 h in the dark to ensure complete equilibration of adsorption/desorption of the organic compound on the catalyst surface. BPA dark adsorption never exceeded 10% of its initial concentration. After that period of time, the suntest lamp and/or the sonicator were turned on, and this was taken as time zero for the reaction. Reaction sets were sampled periodically and filtered with 0.45 μm Millipore filters for H_2O_2, HPLC and DOC analyses. The runs were carried out at least by duplicate. The uncertainties were found lower than 2, 5 and 7% for figures reporting H_2O_2, HPLC and DOC evolution, respectively.

2.3. Analyses

A Shimadzu TOC-Vcsn analyzer was used for dissolved organic carbon (DOC) measurements. The instrument was equipped with an ASI automatic sample injector and a solution of potassium phthalate was used as the calibration standard. Acidification and stripping were carried out before analyses to keep the solutions free of atmospheric CO_2. The concentrations of the pollutant were measured by HPLC in a Shimadzu LC-2010A instrument. A Nucleosil C-18 column (i.d. = 4.6 mm, length = 250 mm) and a UV detector set at 254 or 273 nm were used. The mobile phase, 0.17 mol L^{-1} acetic acid/acetonitrile (60/40%) was run in isocratic mode. Identification of primary BPA intermediates was made by HPLC–MS through a Waters 2695 and a Q-Tof Ultima Waters. Byproduct aliphatic acids were identified by HPLC using a Sarasep CAR-H column, a UV detector set at 210 nm and a 4.8 mmol L^{-1} sulphuric acid solution as the mobile phase.

Hydrogen peroxide concentrations were determined iodometrically [31]. Aliquots taken from the reactor were added in the sample quartz cuvette of the spectrophotometer (Shimadzu, UV-1601) containing the reagent (potassium iodide, 0.1 M and ammonium heptamolybdate, 0.01 M). Absorbance was recorded at 5 min.

3. Results and discussion

3.1. BPA elimination and mineralization by TiO_2 photocatalysis

In photocatalytic processes, TiO_2 dosage is an important parameter that can affect the degradation rate of organic pollutants. Fig. 2 shows both BPA elimination and mineralization as a function of the catalyst concentration under simulated solar illumination. As shown in Fig. 2, after 75 min, the solar light action reduces BPA concentration by 4%, while no removal of DOC was observed after 4 h of irradiation. These results illustrate the low light absorption of BPA in the solar spectrum. When TiO_2 concentration increased from 0 to 0.05 g L^{-1}, a significant enhancement of efficiency was noted for BPA elimination and mineralization. Between 0.05 and 1 g L^{-1} of TiO_2 loading, no significant changes were seen in BPA elimination, whereas the efficiency of DOC removal continued to increase. The number of active surface sites increases with TiO_2 concentration. Thus, the results indicate that at concentrations between 0.05 and 1 g L^{-1}, BPA competes with its degradation intermediates for these active sites on the

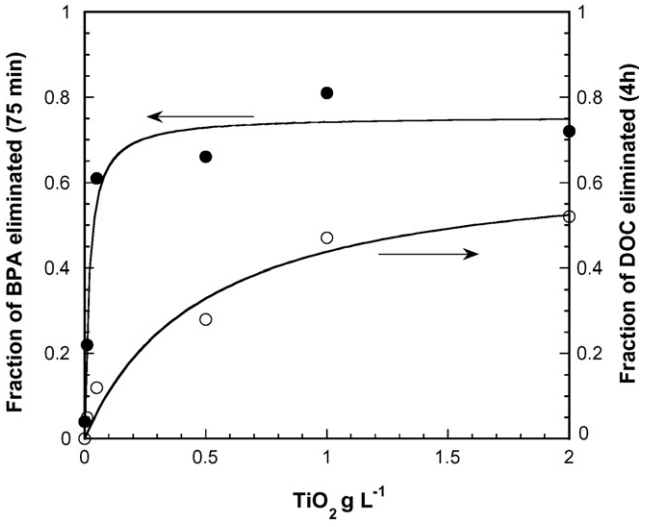

Fig. 2. Photocatalytic BPA elimination after 75 min and mineralization after 4 h at different TiO_2 concentrations (0, 0.01, 0.05, 0.5, 1, and 2 g L^{-1}). The system used 600 mL of BPA at 118 μmol L^{-1}, pH 3, oxygen-saturated solutions and a temperature 22 ± 2 °C.

catalyst surface. Above 1 g L^{-1} of TiO_2, the mineralization rate is slightly influenced by the progressive increase of catalyst concentration. This can be due to both reduction of light penetration and aggregation of TiO_2 particles at relative high catalyst loading. Using 1 g L^{-1} of TiO_2, which is the best compromise between higher efficiency (for BPA and DOC removal) and lower TiO_2 loading, ~100% of BPA (data not shown) and 50% of DOC were eliminated after 4 h of treatment.

3.2. BPA elimination and mineralization by ultrasound

In previous work, we studied the sonochemical degradation of BPA [28]. The best performance was found using a frequency of 300 kHz and an oxygen-saturated solution. Fig. 3 shows the evolution of the substrate, DOC and H_2O_2 during the ultrasonic treatment of a 118 μmol L^{-1} BPA solution at 300 kHz and 80 W. After 2 h of treatment, BPA concentration is lower than the HPLC detection limit. At the same time, ~95% of DOC remains in solution. After 4 h, only 6% of the initial DOC has been removed. This indicates that, in contrast to the initial substrate, BPA byproducts are poorly eliminated by the ultrasonic action. Fig. 3 also shows that hydrogen peroxide is produced during the sonochemial water treatment, primarily from hydroxyl radical recombination. Its concentration, in the absence of substrate, increases linearly with a formation rate of 162 μmol h^{-1} L^{-1}. In the presence of BPA, a lower formation rate is observed (101 μmol h^{-1} L^{-1}), indicating that a fraction of $^{\bullet}OH$ formed reacts with the pollutant. Because of the hydrophobic and slightly volatile character of BPA, $^{\bullet}OH$ attack on BPA is mainly carried out at the interface of the cavitation bubble.

3.3. Comparison of the TiO_2 photocatalytic and 300 kHz ultrasonic systems for BPA treatment in water

Fig. 4 compares the results of the sonochemical and photocatalytic actions on both DOC and BPA removal. Experiments were realized using the same reactor geometry, total volume, pH and oxygen-saturated solutions. The ultrasound

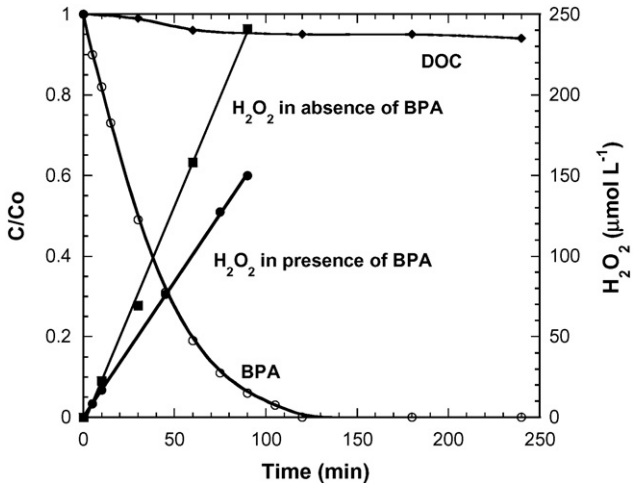

Fig. 3. BPA (118 μmol L^{-1}) elimination, DOC removal and H_2O_2 evolution in the presence and in absence of substrate during sonication (300 kHz; 80 W) of oxygenated solutions. Volume 600 mL; pH 3; temperature 22 ± 2 °C.

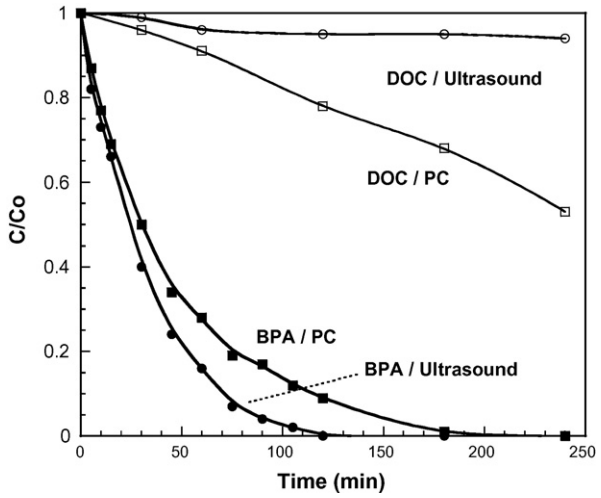

Fig. 4. BPA and DOC removal during sonication (300 kHz; 80 W) or photocatalysis (1 g L^{-1} of TiO_2). BPA concentration 118 μmol L^{-1}; volume 600 mL; pH 3; temperature 22 ± 2 °C; saturating gas is oxygen.

experiment was carried out at the same conditions as in Section 3.2, while the photocatalysis experiment was carried out using 1 g L^{-1} of TiO_2.

In this work, a comparison between photocatalytic and ultrasonic processes cannot be made from the kinetic point of view, since the set-up for each system does not represent the state of the art of each technology. However, certain qualitative trends of the results obtained with each process can be compared. For example, BPA is practically eliminated after 2 and 3 h using ultrasound and photocatalysis, respectively. After 4 h, while ~50% of the initial DOC was removed by photocatalysis, only 6% was eliminated using ultrasound. Thus, under the conditions used, ultrasound is more efficient for eliminating the initial substrate, while photocatalysis is much better for degrading intermediate compounds (DOC removal).

To illustrate these results, Fig. 5 represents the chromatograms of the two AOPs at ~50% of BPA elimination. As can be seen, both systems lead to the same BPA byproducts. Analysis by HPLC–MS in positive electrospray mode showed the formation

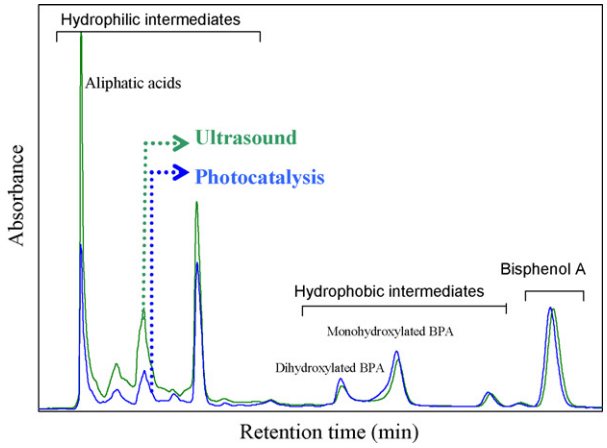

Fig. 5. Chromatograms at 254 nm after 50% of BPA elimination by ultrasound and photocatalysis. Ultrasound: 300 kHz; 80 W. Photocatalysis: 1 g L^{-1} of TiO_2.

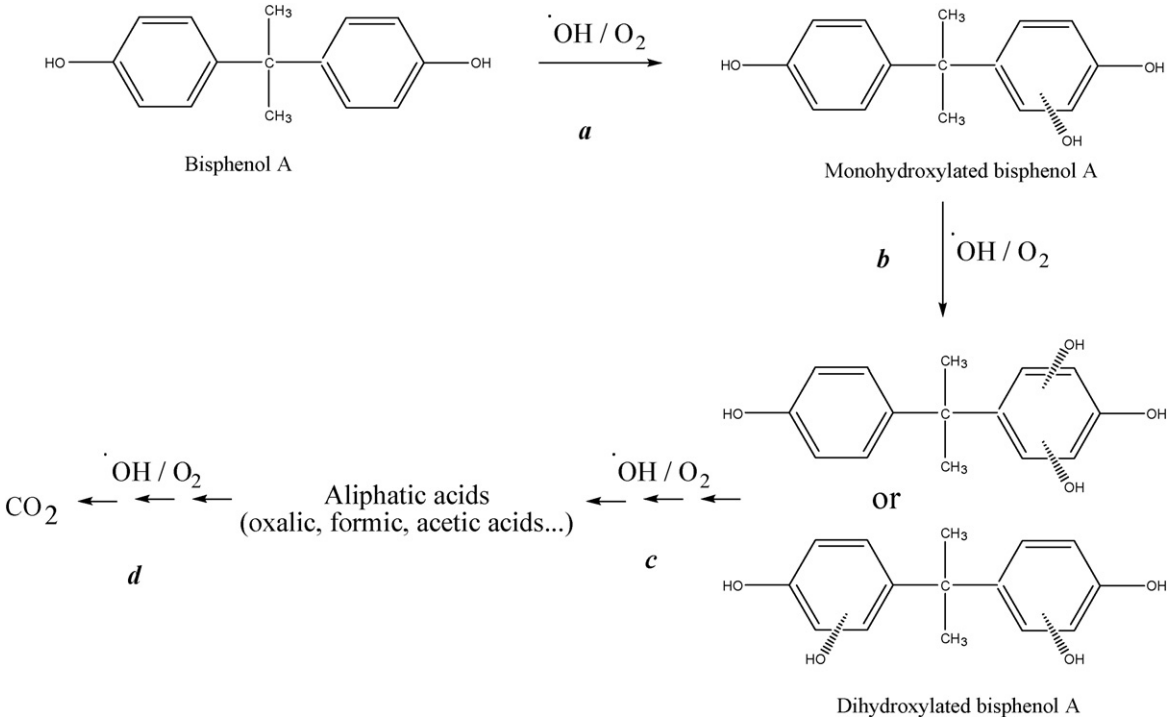

Fig. 6. Main steps during BPA degradation by ultrasound or photocatalysis.

of mono- and di-hydroxylated BPA derivatives. We conclude that the degradation is primarily caused by hydroxyl radical attack in both BPA treatments. Successive attacks of $^{\bullet}OH$ radicals lead to the formation of aliphatic acids such as oxalic, formic and acetic acid. As described earlier, BPA concentrates at the interface during the ultrasonic treatment, where it can be easily degraded by $^{\bullet}OH$ radicals coming from water and oxygen pyrolysis. Unlike the target compound, the more hydrophilic byproducts prefer the solution bulk and thus have low probabilities of reaction with $^{\bullet}OH$ radicals. Because of the short half-life of $^{\bullet}OH$ (10^{-9} to 10^{-6} s), most hydroxyl radicals recombine to produce H_2O_2 rather than reacting with byproducts. In the photocatalytic treatment, the hydrophilic aliphatic acids that are generated, easily adsorb and become decarboxylated on the TiO_2 surface through the photo-Kolbe reaction [32]. This allows a faster degradation compared to the ultrasonic treatment. The last assertion is confirmed by the chromatograms of Fig. 5, showing that the more hydrophilic intermediate compounds, are more recalcitrant to the ultrasonic than to the photocatalytic action. Fig. 6 illustrates the main steps for the BPA degradation by ultrasound or photocatalysis. Our results indicate that steps a and b in Fig. 6 are preferred under ultrasonic action whereas steps c and d are favoured in TiO_2 photocatalysis.

The complementary nature of these two processes makes their combination, discussed in the next section, a promising alternative for the treatment of water contaminated with BPA.

3.4. Coupled photocatalysis and sonication for the bisphenol A treatment

Fig. 7 shows the BPA evolution during both ultrasound and coupled ultrasound/photocatalysis at different TiO_2 loading (0.01–1 g L^{-1}). In all cases, even if photocatalysis slightly enhances the performance of ultrasonic BPA removal, a synergistic effect is not observed. Under all the conditions tested, BPA is practically eliminated after 120 min of treatment.

DOC evolutions for the same experiments as in Fig. 7 are shown in Fig. 8. The results indicate that the combined approach strongly increases the DOC removal of the ultrasonic system. Interestingly, the use of 0.5 g L^{-1} of TiO_2 in the combined system removes less DOC (49%) than 0.05 g L^{-1} (62%). This unexpected result will be discussed later in this section. On the other hand, the mineralization efficiency of the

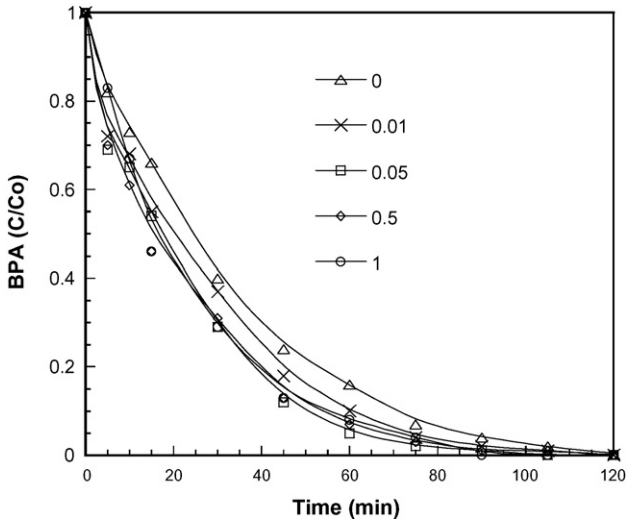

Fig. 7. BPA (118 μmol L^{-1}) evolution during ultrasound (without light) and coupled ultrasound/photocatalysis at different TiO_2 concentrations (0.01–1 g L^{-1}). Volume 600 mL; pH 3; temperature 22 ± 2 °C; oxygen-saturated solutions. Ultrasound: 300 kHz; 80 W.

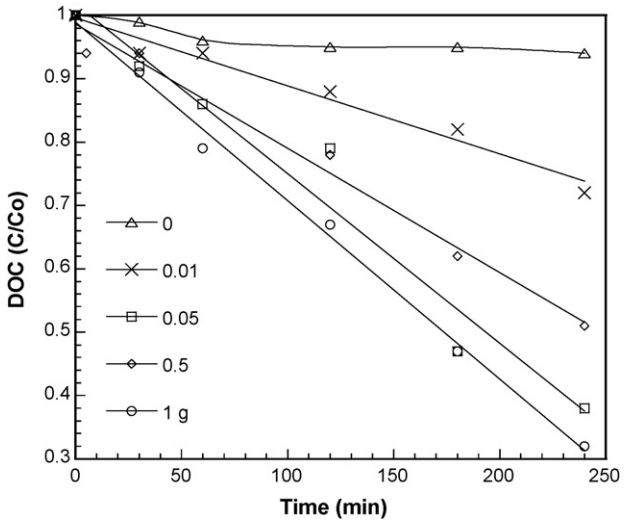

Fig. 8. DOC evolution during BPA (118 μmol L^{-1}) degradation by ultrasound (without light) and ultrasound/photocatalysis at different TiO_2 concentrations (0.01–1 g L^{-1}). Volume 600 mL; pH 3; temperature 22 ± 2 °C; oxygen-saturated solutions. Ultrasound: 300 kHz; 80 W.

combined system with 0.05 g L^{-1} of TiO_2 (62%) is almost as good as using 1 g L^{-1} (68%). Thus, the combined process also offers effective mineralization with low TiO_2 load. This result is in accordance with those of Peller et al. [33] for the mineralization of 2,4-dichlorophenol.

The results observed indicate an interesting synergistic effect between these two AOPs, depending on the catalyst concentration. This synergy (*S*) between ultrasound and photocatalysis, for BPA mineralization, can be better discussed using the following equation:

$$S = \frac{DOC_{ultrasound+photocatalysis}}{DOC_{ultrasound} + DOC_{photocatalysis}} \quad (1)$$

where $DOC_{ultrasound+photocatalysis}$ represents the percentage of DOC removed for the combined process, while $DOC_{ultrasound}$ and $DOC_{photocatalysis}$ represent the percentages of DOC eliminated under ultrasound alone and photocatalysis alone, respectively. If *S* is equal to 1, the effect of combining the two methods is additive; if *S* is higher or lower than 1, the effect is synergistic or antagonistic, respectively. Fig. 9 shows the *S* values after 2 and 4 h for the ultrasonic/photocatalytic treatment at different

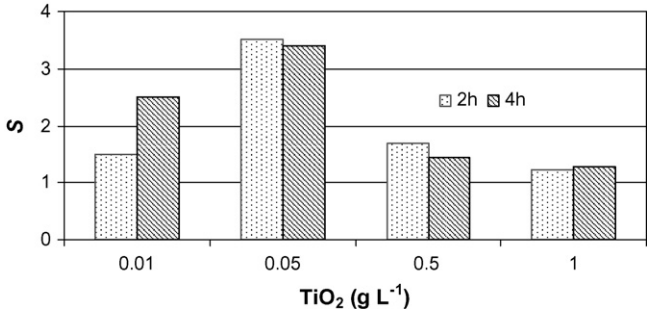

Fig. 9. Influence of TiO_2 loading on the synergistic effect between ultrasound and TiO_2 photocatalysis for BPA mineralization after 2 and 4 h of treatments. The synergy parameter *S* is defined in the text.

TiO_2 loadings. As seen in Fig. 9, after 4 h of treatment, the most pronounced synergistic effect is found at low TiO_2 concentrations. *S* is equal to 2.5 and 3.4 for 0.01 and 0.05 g L^{-1} of TiO_2, respectively, and only 1.3 when 1 g L^{-1} of catalyst is used. Interestingly, the results at 2 h show that the synergy between ultrasound and photocatalysis is also time dependent. For example, using 0.01 g L^{-1} of TiO_2, a synergistic effect of $S = 1.5$ is observed after 2 h of the treatment, and this value rises to 2.5 if the treatment is continued up to 4 h.

Surprisingly, the best catalyst loading for the bare photocatalytic experiments, 1 g L^{-1} of TiO_2 (Fig. 2), presents the worse synergistic effect in the combined system (Fig. 9). Under our conditions, the best synergistic effect for the ultrasonic/photocatalytic system was found using 0.05 g L^{-1} of TiO_2. With this catalyst concentration the combined system removes more than 60% of the initial DOC after 4 h of treatment. This result clearly shows that, to apply a treatment combining ultrasound and photocatalysis for organic removal in water, optimization of each system separately is not the correct approach.

Fig. 10 represents the chromatograms of BPA solutions after 4 h of degradation by ultrasound, photocatalysis and coupled ultrasound/photocatalysis. Photocatalysis and ultrasound/photocatalysis systems were applied using the best TiO_2 loading for the combined process (0.05 g L^{-1}). The results show that, while the TiO_2 photocatalysis process is not able to completely remove either the initial pollutant or the more hydrophobic BPA byproducts, the ultrasonic system is unable to eliminate the more hydrophilic aliphatic acids generated. The combined ultrasound/photocatalysis system, however, benefits from the individual strengths of each process, completely eliminating BPA as well as all the hydrophilic and hydrophobic intermediates. The results confirm that the difference in affinity toward organic compounds of these two processes is a crucial factor to achieve synergistic effects and complete mineralization of organic pollutants.

Other factors, recently reported in the literature, can also explain the performance of the coupled system. These factors can be separated into two groups as follows:

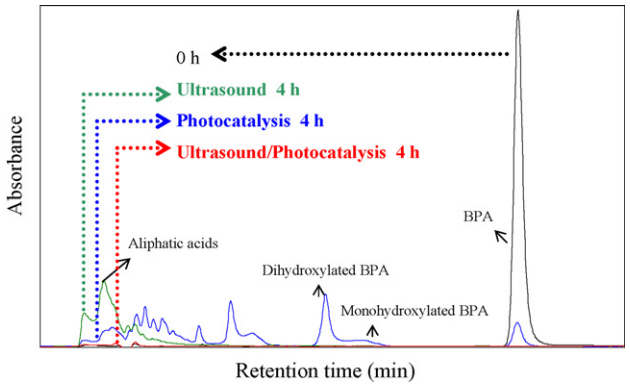

Fig. 10. Chromatograms at 273 nm for BPA (118 μmol L^{-1}) degradation by ultrasound (300 kHz; 80 W), photocatalysis (0.05 g L^{-1} of TiO_2) and ultrasound/photocatalysis (300 kHz; 80 W; 0.05 g L^{-1} of TiO_2) after 4 h of treatments. Volume 600 mL; pH 3; temperature 22 ± 2 °C; saturating gas: oxygen.

(A) Action of ultrasound toward photocatalysis:

(A1) Increases the catalyst surface area due to the de-aggregation action of ultrasound. This enhances the performance of the photocatalytical system [17].

(A2) Improves mass transfer of organic compounds between the liquid phase and the TiO_2 surface [34].

(A3) Reduces the charge recombination and promotes the production of additional $^{\bullet}OH$ due to the residual H_2O_2 generated. H_2O_2 is a better electron acceptor than oxygen [35]:

$$TiO_2(e^-) + H_2O_2 \rightarrow TiO_2 + {}^{\bullet}OH + {}^{-}OH \quad (2)$$

However, if the hydrogen peroxide concentration is relatively high, H_2O_2 may scavenge both hydroxyl radicals and valence band holes:

$$TiO_2(h^+) + H_2O_2 \rightarrow TiO_2 + O_2 + 2H^+ \quad (3)$$

$$^{\bullet}OH + H_2O_2 \rightarrow H_2O + HO_2^{\bullet} \quad (4)$$

(B) Action of photocatalysis toward ultrasound:

(B1) Increases organic degradation due to the TiO_2 particles, providing extra nuclei for bubble formation [36]. Nevertheless, a detrimental effect on sonolytical efficiency may take place because of sound attenuation [17].

Factors A1 and A2 play a larger role at lower catalyst loadings and can explain the higher synergy found at low TiO_2 concentrations.

In order to investigate the role of the factor A3 in the synergistic effect between ultrasound and photocatalysis for mineralization of organic pollutants, we monitored the hydrogen peroxide formation in the absence of pollutant under ultrasound and a solar simulator lamp at different TiO_2 loading levels. As shown in Fig. 11A, without catalyst, a hydrogen peroxide formation rate of 156 μmol h^{-1} L^{-1} is obtained. The ultrasound/photocatalysis process with 0.01 g L^{-1} of TiO_2 produces an insignificant effect on the hydrogen peroxide accumulation. For greater TiO_2 loadings, the higher the TiO_2 concentration, the lower the accumulated H_2O_2. Surprisingly, this trend is not accompanied by a better synergy between the processes (Figs. 7–9). To understand this phenomenon and the role of the factor B1 in the synergy between ultrasound and photocatalysis, Fig. 11B shows the H_2O_2 concentration during water sonication in the absence of light (dark conditions). At these conditions, the catalyst surface cannot be activated and thus hydrogen peroxide produced by ultrasound is not consumed by TiO_2. The results show that, while 0.01 and 0.05 g L^{-1} of TiO_2 have a weak effect on the cavitational activity of ultrasound, 0.5 and 1 g L^{-1} of TiO_2 produce a similar detrimental effect. This negative effect of relatively high quantities of TiO_2 on the cavitational activity was also recently found by Berberidou et al. [17] in the malachite green degradation by sonophotocatalysis. The effect can be attributed to sound attenuation by TiO_2 particles.

Based on the data, the optimal catalyst loading for organic mineralization in the coupled ultrasound/photocatalysis system

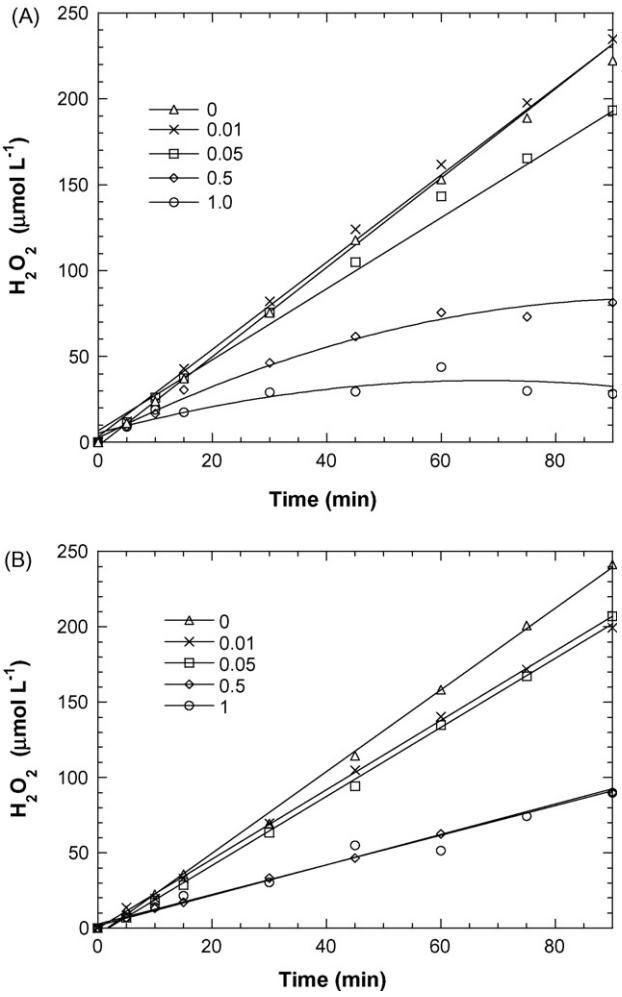

Fig. 11. Evolution of hydrogen peroxide produced by ultrasound (300 kHz, 100 W) applied to water saturated with oxygen at different TiO_2 concentrations (0, 0.01, 0.05, 0.5, and 1 g L^{-1}). Volume 600 mL; pH 3; temperature 22 ± 2 °C. (A) In the presence of light; (B) under dark conditions.

is the concentration that maximizes the beneficial ultrasound actions toward photocatalysis and minimizes the detrimental effects on the cavitation. Also taking into account the performances of the individual processes, 0.05 g L^{-1} is the optimal catalyst load among the TiO_2 concentrations tested for BPA mineralization in the ultrasound/photocatalysis system.

4. Conclusions

Our results demonstrate that high-frequency ultrasound and photocatalysis are complementary processes for pollutant degradation. Since hydrophobic compounds are easily degraded by ultrasound, and hydrophilic compounds are rapidly eliminated by photocatalysis, a system combining both of them constitutes a promising alternative for the complete elimination of an organic chemical such as BPA. The combined approach must be optimized in situ rather than optimizing each process separately. Special attention should be given to the choice of the catalyst concentration in order to ensure that the photocatalysis component of the system benefits from the ultrasonic action

without generating a detrimental effect on the cavitational activity.

Acknowledgements

The authors wish to express their gratitude to the Cooperation@EPFL in the framework of the Colombo-Swiss action and the Rhône-Alpes Region for financial support to Mr. Torres, and to the Federal Commission for Scholarships for Foreign Students of the Swiss Government for the fellowship to Miss Nieto.

References

[1] D. Bahnemann, J. Cunningham, M.A. Fox, E. Pelizzetti, P. Pichat, N. Serpone, in: G.R. Helz, R.G. Zepp, D.G. Crosby (Eds.), Aquatic and Surface Photochemistry, Ed. Lewis Publishiers, Boca Raton, 1994, pp. 261–316.
[2] C. Pulgarin, J. Kiwi, Chimia 50 (1996) 50–55.
[3] A.G. Rincon, C. Pulgarin, J. Sol. Energy Eng. 129 (2007) 100–110.
[4] J. Hoigne, Water Sci. Technol. 35 (1997) 1–8.
[5] R.A. Torres, C. Pétrier, E. Combet, F. Moulet, C. Pulgarin, Environ. Sci. Technol. 41 (2007) 297–302.
[6] Y.G. Adewuyi, Environ. Sci. Technol. 39 (2005) 8557–8570.
[7] R.A. Torres, V. Sarria, W. Torres, P. Peringer, C. Pulgarin, Water Res. 13 (2003) 3118–3124.
[8] J. Bandara, C. Pulgarin, P. Peringer, J. Kiwi, J. Photochem. Photobiol. A 111 (1997) 253–263.
[9] M.R. Hoffmann, I. Hua, R. Höchemer, Ultrason. Sonochem. 3 (1996) S163–S172.
[10] C. Pétrier, D. Casadonte, in: T.J. Mason, A. Tiehm (Eds.), Advances in Sonochemistry: Ultrasound in Environmental Protection, Vol. 6, JAI Press Inc., Stamford, 2001, pp. 91–109.
[11] H. Okuno, B. Yim, Y. Mizukoshi, Y. Nagata, Y. Maeda, Ultrason. Sonochem. 7 (2000) 261–264.
[12] T.J. Mason, C. Pétrier, in: S. Parson (Ed.), Advanced Oxidation Processes for Water and Wastewater treatment, IWA Publishing, London, 2004, pp. 185–208.
[13] J. Peller, O. Wiest, P.V. Kamat, J. Phys. Chem. A 105 (2001) 3176–3181.
[14] D. Bahnemann, Sol. Energy 77 (2004) 445–459.
[15] S. Malato, J. Blanco, D.C. Alarcón, M.I. Maldonado, P. Fernández-Ibáñez, W. Gernjak, Catal. Today 122 (2007) 137–149.
[16] P. Théron, P. Pichat, C. Guillard, C. Pétrier, T. Chopin, Phys. Chem. Chem. Phys. 1 (1999) 4663–4668.
[17] C. Berberidou, I. Poulios, N.P. Xekoukoulotakis, D. Mantzavinos, Appl. Catal. B 74 (2007) 63–72.
[18] M. Mrowetz, C. Pirola, E. Selli, Ultrason. Sonochem. 10 (2003) 247–254.
[19] E. Selli, Phys. Chem. Chem. Phys. 4 (2002) 6123–6128.
[20] N. Stock, J. Peller, K. Vinodgopal, P.V. Kamat, Environ. Sci. Technol. 34 (2000) 1747–1750.
[21] T. Yamamoto, A. Yasuhara, H. Shiraishi, O. Nakasugi, Chemosphere 42 (2001) 415–418.
[22] M. Furhacker, S. Scharf, H. Weber, Chemosphere 41 (2000) 751–756.
[23] C.A. Staples, P.B. Dorn, G.M. Klecka, S.T. O'Block, L.R. Harris, Chemosphere 36 (1998) 2149–2173.
[24] G.V. Korshin, J. Kim, L. Gan, Water Res. 40 (2006) 1070–1078.
[25] J.Y. Hu, T. Aizawa, S. Ookubo, Environ. Sci. Technol. 36 (2002) 1980–1987.
[26] R. Kuruto-Niwa, Y. Terao, R. Nozawa, Environ. Toxicol. Pharmacol. 12 (2002) 27–35.
[27] A.G. Chakinala, P.R. Gogate, A.E. Burgess, D.H. Bremner, Ultrason. Sonochem. 14 (2007) 509–514.
[28] R.A. Torres, C. Pétrier, E. Combet, C. Pulgarin, Ultrason. Sonochem. 15 (2008) 605–611.
[29] C. Pétrier, M.F. Lamy, A. Francony, A. Benahcene, B. David, V. Renaudin, N. Gondrexon, J. Phys. Chem. 98 (1994) 10514–10520.
[30] T.J. Mason, J.P. Lorimer, D.M. Bates, Ultrasonics 30 (1992) 40–42.
[31] C. Kormann, D.W. Bahnemann, M.R. Hoffmann, Environ. Sci. Technol. 22 (1988) 798–806.
[32] M.I. Franch, J.A. Ayllón, J. Peral, X. Doménech, Catal. Today 76 (2002) 221–233.
[33] J. Peller, O. Wiest, P.V. Kamat, Environ. Sci. Technol. 37 (2003) 1926–1932.
[34] T.J. Mason, J.L. Luche, Chemistry under Extreme or Non-Classical Conditions, John Wiley & Sons, New York, 1997, p. 317.
[35] R. Diller, I. Fornefett, U. Siebers, D.W. Bahnemann, J. Photochem. Photobiol. A 96 (1996) 231–236.
[36] T. Tuziuti, K. Yasui, Y. Iida, H. Taoda, S. Koda, Ultrasonics 42 (2004) 597–601.